Structural Engineering and Mechanics, Vol. 8, No. 1 (1999) 27-38
DOI: http://dx.doi.org/10.12989/sem.1999.8.1.027

Effect of cable stiffness on a cable-stayed bridge

Yang-Cheng Wang†

Department of Civil Engineering, Chinese Military Academy,
1 Hwang-Poo Road, Feng-Shan, 83000, Taiwan, R.O.C.

Abstract. Cables are used in many applications such as cable-stayed bridges, suspension bridges, transmission lines, telephone lines, etc. Generally, the linear relationship is inadequate to present the behavior of cable structure. In finite element analysis, cables have always been modeled as truss elements. For these types of model, the nonlinear behavior of cables has been always ignored. In order to investigate the importance of the nonlinear effect on the structural system, the effect of cable stiffness has been studied. The nonlinear behavior of cable is due to its sag. Therefore, the cable pretension provides a large portion of the inherent stiffness. Since a cable-stayed bridge has numerous degrees of freedom, analytical methods at present are not convenient to solve this type of structures but numerical methods may be feasible. It is necessary to provide a different and more representative analytical model in order to present the effect of cable stiffness on cable-stayed bridges in numerical analysis. The characteristics of cable deformation have also been well addressed. A formulation of modified modulus of elasticity has been proposed using a numerical parametric study. In order to investigate realistic bridges, a cable-stayed bridge having the geometry similar to that of Quincy Bayview Bridge is considered. The numerical results indicate that the characteristics of the cable stiffness are strongly nonlinear. It also significantly affects the structural behaviors of cable-stayed bridge systems.

Key words: characteristics; cable stiffness; cable-stayed bridge.

1. Introduction

Cable-stayed bridge systems can be divided into several primary components such as the cable system, the stiffening girders, the bridge deck and the pylons. The nonlinearity of cable-stayed bridges depends on the behaviors of cables, pylons, the bridge deck and their interactions. A large cable-stayed bridge system has a large number of cables. The nonlinearity of cables is one of the most important factors of the structural behaviors. Agrawal (1997) indicated that the number of cables not only changes the axial forces acting on the bridge deck but also changes the moments along the bridge deck. The nonlinear behavior of a cable is due to its sag. With an increasing axial load, the elongation of the cable is increased but the total cable sag is decreased. The factors which may affect the nonlinear behavior such as the cable tension, the cable's own weight and different geometries, etc., are investigated. Agrawal investigated the effect of number of cables on the behavior of cable-stayed bridges. He indicated that maximum cable tension and the weight of steel decreased rapidly with the increase in the number of cables. The weight of steel in cable-stayed bridges could vary substantially with variation of cable stiffness or flexure rigidity of the

† Associate Professor and Chairman

girders. The cables away from the tower are more effective in supporting the load. Shu and Wang (1997) indicated that due to the vertical component of the cable tension acting on the pylon coupled with the bending moments, the pylon has nonlinear behavior. Agrawal also indicated that the girder moments are larger in the case of bridges having larger numbers of cables. The girder moments in these bridges decrease sharply with the increase of cable rigidity. The cable stiffness significantly affects the behavior of cable-stayed bridges. Wang and Hua (1998) indicated that the different locations and number of cables would also change the stiffness of the cable-stayed bridges. Under stability analysis, the critical loads of cable-stayed bridges were significantly changed due to the cable stiffness.

2. Description of the structures and idealizations

Cable-stayed bridges use cables instead of piers to support the bridge deck as the interval supports. The cables provide a large portion of stiffness in the cable-stayed bridges. Due to the nonlinear behavior of cables, cable-stayed bridges have larger nonlinearity compared to that of conventional continuous bridges. In order to study the nonlinear behavior of cable-stayed bridges, the nonlinear behavior of cables must be investigated. The deformation characteristics of a single cable, which is based on cantenary profile (Beer and Johnston 1995 and Broughton and Ndumbaro 1994), have been provided. To investigate the cable stiffness effects on realistic cable-stayed bridges, a bridge having geometry similar to that of the Quincy Bayview Bridge has been studied.

2.1. Description of the structures

The Quincy Bayview Bridge was designed by Mojeski and Mater (1983) and completed in 1987 as a cable-stayed bridge across the Mississippi River at Qunicy, Illinois, USA. The Quincy Bayview Bridge has 25 different cross sectional areas of the 56 cables, two H-type pylons and a 46.5ft (1ft=0.3048 m) wide composite steel and concrete girder deck. The bridge has one main span and two side spans. The main span length is 900ft. Each side span length is 440ft. The total length of the bridge is 1780ft. The cross sectional areas of the cables range from 4.07 in^2 to 13.892 in^2 (1 in^2=645.2 mm^2). Table 1 shows the cross sectional area of cables. The cables are numbered from 1 to 14 from the side span to the midspan of west as well as east pylons (Fig. 1). The

Table 1 The cross section areas of cables

West (left) tower				East (right) tower			
Cable #	Cross sec. area (in^2)	Cable #	Cross sec. area (in^2)	Cable #	Cross sec. area (in^2)	Cable #	Cross sec. area (in^2)
1	13.892	2	13.892	14	10.554	13	10.161
3	11.437	4	10.161	12	8.9340	11	7.9520
5	6.7740	6	5.6450	10	6.5780	9	5.1540
7	4.3690	8	4.0740	8	4.1230	7	4.3200
9	5.1050	10	6.4800	6	5.4890	5	6.7250
11	7.8540	12	8.7870	4	10.014	3	11.290
13	10.063	14	10.505	2	13.892	1	13.892

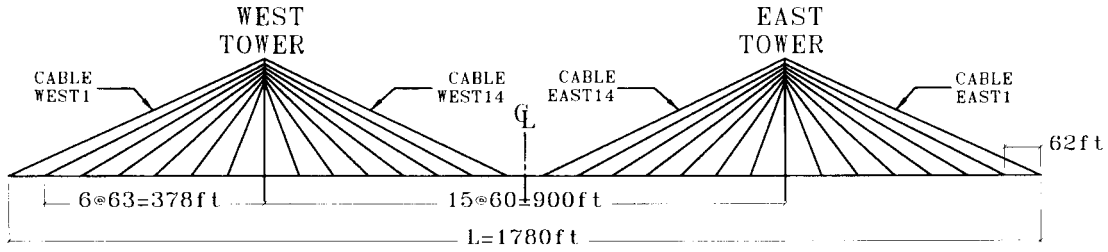

Fig. 1 The geometry and cable number of Quincy Bayview Bridge

inclination of the cables with deck varies from 38.3° to 69.3°. Twenty-eight cables support the main span and 14 cables support each side span. The cables are connected at the bottom flange of the main girder. The cables are attached to the pylons at 9-ft interval beginning at 6 ft from the top of the pylon. The cables are symmetrical in the longitudinal direction.

2.2. Idealization

In order to make the results more realistic, the following assumptions were made:
(i) Members are initially straight and piecewise prismatic.
(ii) The material is linearly elastic and the original moduli of elasticity E in both the tension and compression are equal.
(iii) The effect of residual stresses is negligibly small.
(iv) The steel used is isotropic, linearly elastic with modulus of elasticity E as 3.0×10^7 psi (1 psi =6.895 kPa) and Poisson's ratio v as 0.3. The unit weight is 490 lb/ft^3 (1 lb/ft^3=16.0 kg/m^3).
(v) There is no effect on the material properties due to temperature variations.
(vi) The modulus of elasticity of concrete E is taken as 4.47×10^6 psi, Poisson's ratio v as 0.25 and the unit weight as 150 lb/ft^3.

3. Deformation characteristics of a single cable

In order to enable the cable-stayed bridge deck and girders to span a longer distance, high strength cables have been used instead of internal supports. In general, the bridge can be investigated on the assumption that the cables are completely flexible and resist only the tensile forces. Understanding the deformation characteristics of a single cable is essential to analyze the effect of cable behavior on cable-stayed bridges. The nonlinear behavior of an individual cable is due to its sag caused by its own weight and external loads. The cable can be considered as a weightless element subjected to a uniform load. The geometry and the free body diagram of a cable subjected to its own weight are presented in Fig. 2(A) and (B), respectively. Based on the assumption, cable's profile function, $y(x)$, is derived. If μ is the cable's weight per unit length, the variation of the vertical resultant is

$$dR = \mu ds \tag{1}$$

In order to find an equivalent uniform vertical load, set

$$dR = w_e dx = \mu ds \Rightarrow w_e = \mu \frac{ds}{dx} \tag{2}$$

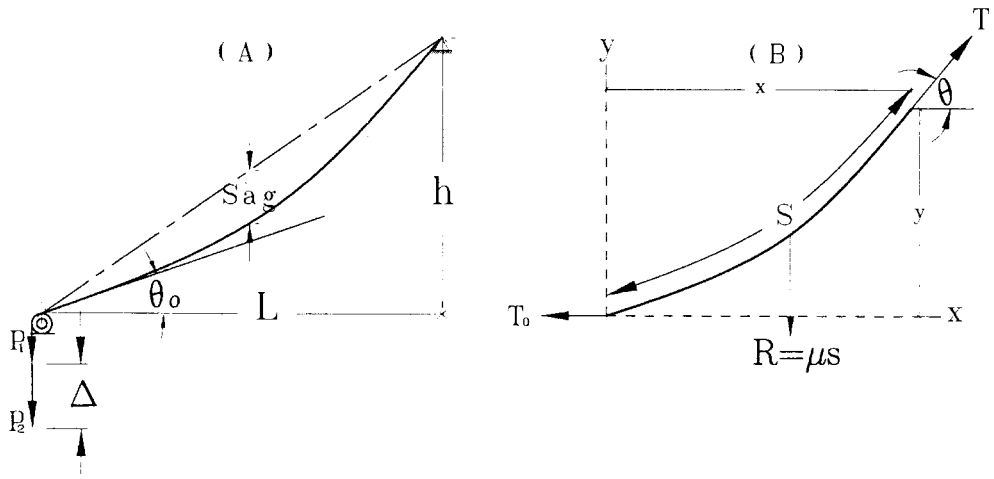

Fig. 2 (A) The geometry of a single cable; (B) The free body diagram

where w_e is the unit weights per unit horizontal length. In this case, the equivalent equation can be written as

$$\frac{d^2y}{dx^2} = \frac{w_e}{T_o} = \frac{\mu \dfrac{ds}{dx}}{T_o} \tag{3}$$

where T_o is horizontal components of cable axial force at the lower end. Rewriting Eq. (3),

$$\frac{d^2y}{dx^2} = \frac{\mu}{T_o}\frac{ds}{dx}$$

Since

$$(ds)^2 \simeq (dx)^2 + (dy)^2 \quad \text{or} \quad \frac{(ds)^2}{(dx)^2} = 1 + \frac{(dy)^2}{(dx)^2} \quad \text{or} \quad \frac{ds}{dx} = \sqrt{1 + \frac{(dy)^2}{(dx)^2}} \tag{4}$$

Thus, the above equation can be written as

$$\frac{d^2y}{dx^2} = \frac{\mu}{T_o}\sqrt{1 + \frac{(dy)^2}{(dx)^2}}$$

Integrate the above equation twice and get

$$\Rightarrow y(x) = \frac{T_o}{\mu}\cosh\left(\frac{\mu}{T_o}x + c\right) + d \tag{5}$$

In order to determine the integral constants (c and d), apply the boundary conditions in the Eq. (5). Let the cable have coordinates (0, 0) at the lower end and (L, h) at the upper end. Then, Eq. (5) can be rewritten as

$$y\,|_{x=0} = 0 \Rightarrow y(0) = \frac{T_o}{\mu}\cosh(c) + d = 0 \tag{6}$$

$$y|_{x=L} = h \Rightarrow y(L) = h = \frac{T_o}{\mu}\left[\cosh\left(\frac{\mu L}{T_o} + c\right)\right] + d \tag{7}$$

Thus, the integral constants (c and d) can be determined using Eqs. (6) and (7). Eliminating d, one has $\frac{T_o}{\mu}\left[\cosh\left(\frac{\mu}{T_o}L + c\right) - \cosh(c)\right] - h = 0$ which can be solved for c numerically (i.e., Newton method) for a given set of h and L. A single cable has different profiles if it is subjected to different external loads. For a numerical example, let a cable have the horizontal width (L) of 5,280 in (1 in=25.4 mm), the vertical height (h) of 2,248 in, cross-sectional area (A) of 27.784 in^2 and modulus of elasticity (E) of 3.0×10^7 psi. Fig. 3(A) represents the different cable profiles due to different values of T_o, 60,000 lb (1 lb=0.4536 kg), 100,000 lb, 200,000 lb and 300,000 lb. The horizontal and vertical axes of Fig. 3(A) represent the horizontal and vertical distances of the cable, respectively.

Fig. 3(A) indicates that the cable profiles will be significantly changed as T_o is changed. To illustrate the relationship between the cable sag and the applied load, Fig. 3(B) represents the maximum cable sag. Fig. 3(B) clearly indicates that the relationship between the horizontal component of applied load and the maximum sag of the cable is nonlinear. In order to precisely investigate this nonlinear behavior, the load-displacement curve must be drawn. In determination of the cable load-displacement curve, the total length of cable, S, and the relationship between T_o and P (the axial cable tension force at the lower end) must be computed. The total length of cable S can be found using numerical methods. Based on Eq. (5) and $(ds)^2 \simeq (dx)^2+(dy)^2$, S can be estimated as

$$S = \sum_{i=1}^{n} \sqrt{(x_i - x_{i-1})^2 + (y_i - y_{i-1})^2} \tag{8}$$

where i=1, 2, ⋯, n and n is the number of horizontal divisions (the horizontal length is divided into n segments). In determination of the total cable length (S), the procedure requires the following steps:

1. Assume T_o, h and L.
2. Numerically solve $\frac{T_o}{\mu}\left[\cosh\left(\frac{\mu}{T_o}L + c\right) - \cosh(c)\right] - h = 0$ in order to determine the integral constant (c) of the cable profile function.
3. Compute the initial tangent angle θ_o where $\tan\theta_o = \frac{dy}{dx}|_{x=0} = \sinh(c)$.
4. Compute the integral constant, $d = -\frac{T_o}{\mu}\cosh(c)$.
5. Plot the cable profile $y(x) = \frac{T_o}{\mu}\cosh\left(\frac{\mu}{T_o}x + c\right) + d$.
6. Calculate total length of the cable $S = \sum\sqrt{(dx)^2+(dy)^2}$.
7. Set $T_o = T_o + dT_o$ and repeat steps 2-7 if necessary.

To determine the relationship of the cable force at the lower end (P) and its horizontal

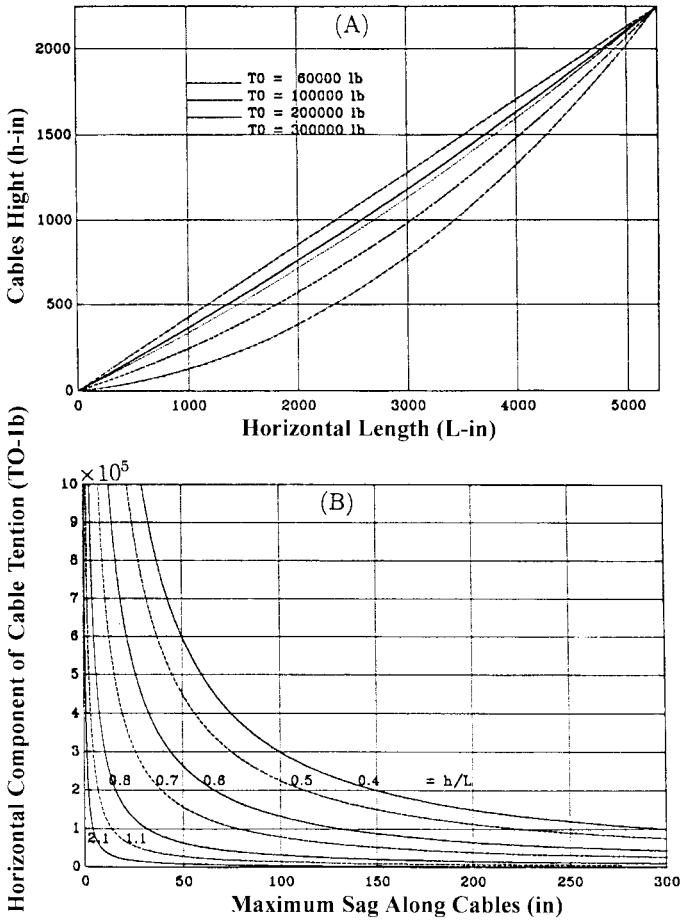

Fig. 3 (A) Cable profiles; (B) Applied load versus the maximum cable sag

component (T_o), the initial angle (θ_o) must be computed. The initial angle is defined as

$$\tan\theta_o = \frac{dy}{dx}\Big|_{x=0} \tag{9}$$

The derivation of the cable profile function $y(x)$ uses $\tan\theta_o = (dy/dx)|_{x=0}$. Thus, $\sinh((\mu/T_o)x + c)|_{x=0} = \sinh(c) \Rightarrow \theta_o = \tan^{-1}(\sinh c)$. The initial angle θ_o at the lower end of the single cable is defined as $P = (T_o/\cos\theta_o)$ where $\theta_o = \tan^{-1}(\sinh c)$ as shown in Fig. 3. The integral constant c can be determined by the boundary conditions. In determination of the cable force (T), the cable profile function is used. The tangent angle θ_i at $x=x_i (0 \le x_i \le L)$ is defined as

$$\tan\theta_i = \frac{dy}{dx}\Big|_{x=x_i} \quad 0 \le i \le n$$

Therefore,

$$\tan\theta_i = \sinh\left(\frac{\mu}{T_o} x_i + c\right) \tag{10}$$

Rewriting Eq. (10) as the function of θ_i

$$T_i = \frac{T_o}{\cos\theta_i} \quad \text{where} \quad \theta_i = \tan^{-1}\left[\sinh\left(\frac{\mu}{T_o} x_i + c\right)\right] \tag{11}$$

Eq. (11) represents the function of the axial force along the cable.

4. Cable stiffness

Cable sag and axial forces affect its stiffness. The cable sag changes due to the cable elongation and the geometric change caused by external loads. The elongation is governed by the modulus of elasticity. It is a linear behavior. The geometric change in cable sag excluding the cable elongation is a nonlinear behavior. Based on the above discussion of cable profiles and axial forces along the cable, apparently the cable stiffness depends on the cable axial force. The total length change of the cable including the material and geometric effects are nonlinear.

For numerical examples, Fig. 4 represents the logarithmic plot of load-displacement relationship for all of the cables in the side span of Quincy Bayview Bridge. The horizontal axis represents the logarithmic values of T_o. Fig. 4 indicates that the cables with higher ratio of h_i/L_i have less δ. After the load-displacement curves are obtained, the cable stiffness can be computed using the load-displacement relationship. The cable stiffness (K) is defined as

$$K_i = \frac{S_{i-1} - S_i}{P_i - P_{i-1}} = \frac{\Delta_i}{dP_i} \tag{12}$$

Fig. 5 represents the logarithmic plot of the cable stiffness (K) versus the cable axial force at lower end (P). It indicates that the logarithmic relation between K and P is linear. The logarithmic plots are parallel for all cables having the same properties with various ratios of h/L used in the side span of Quincy Bayview Bridge.

4.1. Load-displacement curve of cable

The relation between the cable sag and the applied load is nonlinear. Load-displacement curves are one of the most important ways to illustrate the nonlinear behavior. Fig. 4 presents the cable load-displacement curves plotted between T_o versus δ_i or P versus δ_i. The load-displacement curves are strongly nonlinear for all the ratios of h/L.

4.2. Cable influence lines

Under normal design load, the range between dead load and total maximum load called Realistic Loading Region of cable is the most interesting for bridge designers. The total maximum load is defined as the summation of dead load and the possible maximum live load. Cable influence lines can be efficiently used in determination of the possible maximum live load. Based on the Müller-Brealau's Principle, a unit relative displacement between the two connections of the bridge deck and the pylon is required to find the cable influence line. It is very difficult to find the relative displacement between the cable connections by applying a corresponding load.

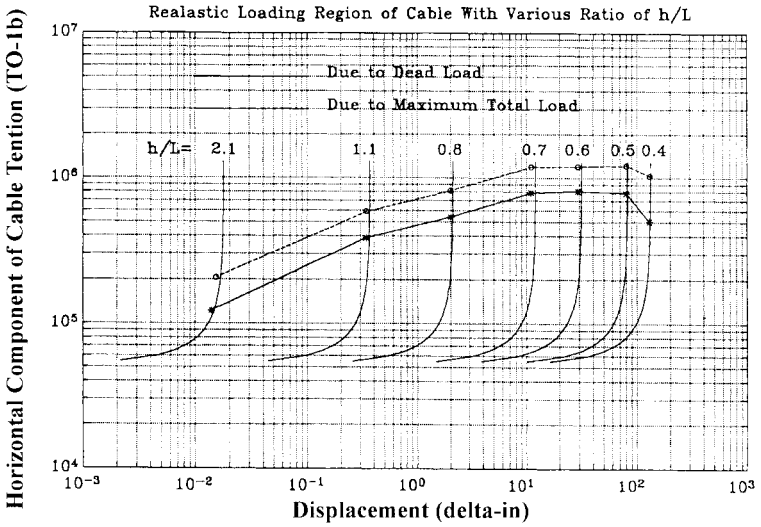

Fig. 4 The logarithmic plot of cable stiffness versus P and the realistic loading region

However, a modified method to find the cable influence lines of cable-stayed bridges is proposed. The method is described in the following steps:

1. Release one cable connection.
2. Apply a unit load at the connections of the bridge deck and the pylon.
3. Compute the deflection of the deck.
4. Normalize the deflections and retain unit relative displacement between the locations at the point of unit load action.
5. Reattach the cable.
6. Repeat steps 1 to 5, if necessary.

4.3. Realistic loading region of cable

Under normal design load, the designers may only be interested in the range between the reaction forces due to dead load and maximum total load. In order to get total maximum load, the load conditions must be determined. The dead load per linear foot of a bridge deck similar to that of Quincy Bayview Bridge is calculated, and it is equivalent to 7,000 lb/ft (1 lb/ft=1.488 kg/m). According to AASHTO (3.8.2.2) (1992), the uniform lane load of 640 lb per linear foot for HS20-44 trucks has been used. The procedure for the determination of the Realistic Loading Region of cable is described in the following steps:

1. The sign convention is defined as under
(1) The areas of the influence lines above the original bridge deck are defined as positive.
(2) The areas of the influence lines below the original bridge deck are defined as negative.
(3) Total positive influence line area is the summation of the positive areas.
(4) Total negative area of the influence line is the summation of the negative areas.
(5) Total influence line area is the summation of the positive and negative influence line areas.
2. Calculate the positive, negative, and total areas of each cable influence line.
3. The effect of dead load of each cable is the total influence line areas of the cable multiplied

by the dead load per unit length (7000 lb/ft).

4. The effect of uniform live load of each cable is the total positive influence line area of the cable multiplied by the uniform live load.
5. The effect of concentrated live load of each cable is only the maximum positive ordinate of the cable influence line multiplied by the concentrated live load.
6. The effect of dead load is the result of step 3, but the maximum total result is the summation of the results of steps 3, 4, and 5.
7. Repeat steps 2 to 5, if the effect of another cable is to be calculated.

Fig. 4 also represents the Realistic Loading Region of the logarithmic plot of load-displacement relationship for all of the side span cables. Fig. 5 also represents the Realistic Loading Region of the logarithmic relationship between cable stiffness K and the horizontal components of the axial force at the lower end P for various ratios of h/L.

5. Modified modulus of elasticity

In finite element models, cable is usually considered as a truss element or number of truss elements connected by their prestress. To investigate the nonlinear behavior of cable, the equivalent modulus of elasticity incorporating the effects of material and change in cable sag should be calculated by a convenient procedure. Modified modulus of elasticity is an efficient method to take care of the partial nonlinearity of the cable. In order to calculate modified modulus of elasticity, the cable displacement function must be determined. Several polynomial functions have been proposed by researchers such as Tang's (1972) equation represented in Eq. (13)

$$(E)_{mod} = (E)_{ori} \frac{1}{1 + \dfrac{G^2 \cos^5\theta (EA)}{12 T_o^3}} \tag{13}$$

where $(E)_{mod}$ is the modified modulus of elasticity, $(E)_{ori}$ is the original modulus of elasticity and G is the total weight of the cable. Different from the exist methodology, in numerical analysis the mathematical expression of the cable displacement used in this paper is

$$\delta = \frac{(P_i - P_{i-1}) L_T}{(E)_{mod} A} = \frac{(P_i - P_{i-1}) S}{(E)_{ori} A} + \Delta \tag{14}$$

If the cross-sectional area remains the same, then the modified modulus of elasticity can be estimated as

$$\left.\begin{aligned} \Rightarrow \frac{L_T}{(E)_{mod}} &= \frac{S}{(E)_{ori}} + \frac{A}{P_i - P_{i-1}} \Delta \\ \Rightarrow (E)_{mod} &= \frac{L_T}{\dfrac{S}{(E)_{ori}} + \dfrac{A}{P_i - P_{i-1}} \Delta} \end{aligned}\right\} \tag{15}$$

Eq. (15) represents the equation of modified modulus of elasticity by using numerical procedure.

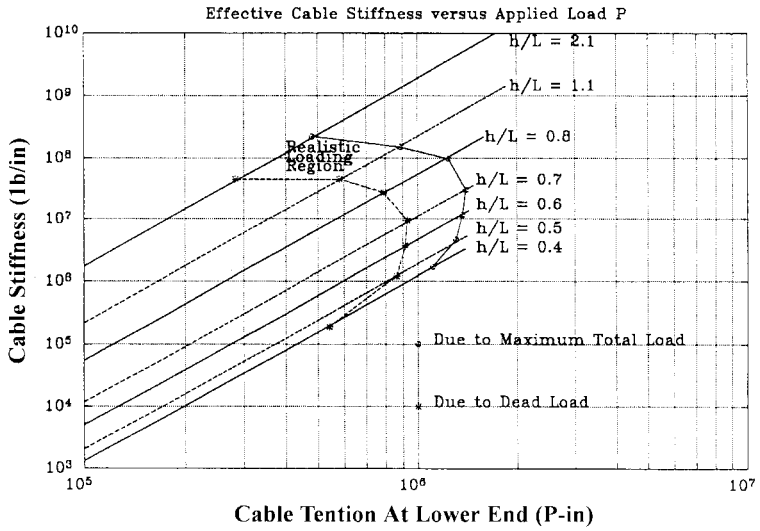

Fig. 5 The logarithmic plot of load-displacement curve of T_0 versus δ and the realistic loading region

6. Numerical results and discussions

In order to investigate the effects of cable stiffness on cable-stayed bridges, an eigen-buckling program has been used to investigate the structural behaviour (Ermopoulos *et al.* 1992 and 1993). Fig. 6 represents the comparison of critical loads with and without modified modulus of elasticity. In Fig. 6, the first buckling load of the bridge without modified modulus of elasticity of the cables is considered as unity. In order to simplify the buckling analysis for designer, the cables of cable-stayed bridges can be modeled as linearly elastic spring to support the bridge deck. The equivalent spring constant can be determined using static analysis. Fig. 7 represents the simple model of the cable-stayed bridge and the first buckling mode. Fig. 7(A) represents the cable-stayed bridge subjected to dead load. Using static analysis, the axial forces acting on the bridge deck due to the cable reaction were found. Fig. 7(B) represents the simple model of the cable-

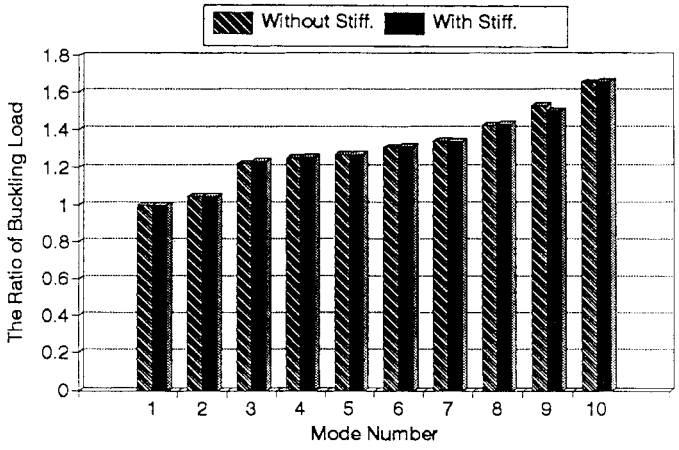

Fig. 6 Comparison of critical load with and without modified modulus of elasticity

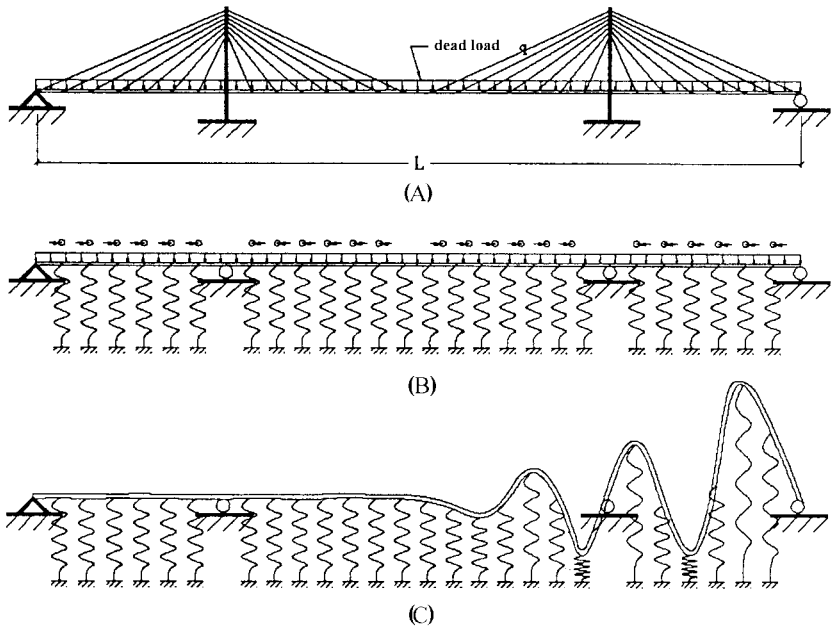

Fig. 7 (A) The original cable-stayed bridge; (B) The simple model of the cable-stayed bridge; (C) The first buckling mode shape of simple model of cable-stayed bridge

stayed bridge. The linearly elastic spring with the equivalent spring constant determined by Fig. 5 and the axial forces acting on the bridge deck were considered instead of the cables. On the other hand, the bridge deck was modeled as a continuous beam subjected to axial forces and supported by the linearly elastic springs. Fig. 7(C) represents the first buckling mode shape of the simple model. This mode shape has a good agreement with that of the first buckling mode shape of the original bridge.

Compared with the critical load of the original bridge, the critical loads of the simple model

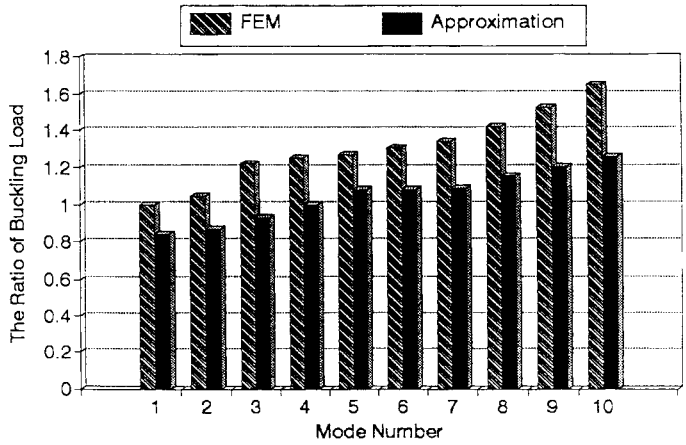

Fig. 8 Comparison of the normalized buckling load for the results obtained by finite element and approximate methods

bridge are approximately 20% underestimated because the simple model bridge lacks interactions between the bridge deck and the pylons. Fig. 8 represents the comparison of the normalized buckling load for the results of finite element methods and approximate method.

7. Conclusions

Based on the analyses in this paper, the important conclusions can be drawn as follows,

1. The cable behavior is strongly nonlinear either subjected to cable's own weight or subjected to external load.
2. By increasing the ratio of h_i/L_i, the cable stiffness increases.
3. The effect of the ratio of h_i/L_i is much more significant than that of the cross-sectional area of the cables.
4. In this type of cable-stayed bridge, the relationship between the logarithmic cable stiffness and the logarithmic cable tension force at the lower end is linear.
5. The stiffness of cables can be estimated effectively using numerical procedures.
6. The cable stiffness, used in this type of bridges, affects significantly the stability analysis.

References

Agrawal, T.P. (1997), "Cable-stayed bridge-parametric study", *Journal of Bridge Engineering, ASCE,* **2**(2), 61-67.

AASHTO (1992), *Standard Specifications for Highway Bridges*, Fifteenth Edition, AASHTO.

Beer, Ferdinand P. and Johnston, E. Russell, Jr. (1995), *Vector Mechanics for Engineers: Static*, Fifth Edition, McGraw-Hill.

Broughton, Peter and Ndumbaro, Paul (1994), *The Analysis of Cable & Cantenary Structures*, Thomas Telford.

Ermopoulos, J. CH., Vlahinos, A.S. and Wang, Y.-C. (1992), "Stability analysis of cable-stayed bridges", *Computers & Structures,* **44**(5), 1803-1809.

Mojeski and Master (1983), "Structural drawing of the Qunicy Bayview Bridge", Mojeski and Master Consulting Engineering, Marrisburg, Pennsylvania.

Shu, H.-S. and Wang, Y.-C. (1997), "Nonlinear static analysis of cable-stayed bridges", *Proceeding of the ANSYS User Conference*, Taiwan, **2**, 1-8.

Tang, M.C. (1972), "Design of cable-stayed girder bridges", *Journal of the Structural Division, ASCE ST8*, 1780-1802.

Vlahinos, A.S., Ermopoulos, J. CH. and Wang, Y.-C. (1993), "Buckling analysis of steel arch bridges", *Journal of Constructional Steel Research,* **26**, 59-71.

Wang, Y.-C. and Hua, C.-H. (1998), "Effects on number of cables for modal analysis of cable-stayed bridges", *Proceedings of the 16th International Modal Analysis Conference*, Feb., 1374-1380.